22P103-P

Study of the Dependence of the Internal Distribution in a Pellet Plasmoid on the Magnetic Field Strength by High-speed Imaging Spectroscopy
高速イメージング分光による高密度プラズマ塊内部分布の磁場強度依存性の研究

Gen Motojima[1)], Ryuichi Sakamoto[1)], Motoshi Goto[1)], Akinobu Matsuyama[1)], Jyoti Shankar Mishra[2)], Hiroshi Yamada[1)] and LHD experiment group[1)]
本島厳[1)], 坂本隆一[1)], 後藤基志[1)], 松山顕之[1)], J.S. Mishra[2)], 山田弘司[1)], LHD実験グループ[1)]

[1)]*National Institute for Fusion Science 322-6 Oroshi-cho, Toki-city, Gifu 509-5292, Japan*
[2)]*The Graduate University for Advanced Studies 322-6 Oroshi-cho, Toki-city, Gifu 509-5292, Japan*
[1)]核融合科学研究所　〒509-5292　岐阜県土岐市下石町322-6
[2)]総合研究大学院大学　〒509-5292　岐阜県土岐市下石町322-6

To investigate the physics of pellet plasmoid dynamics, internal distribution measurements in a pellet plasmoid by high-speed imaging spectroscopy have been demonstrated successfully in the Large Helical Device (LHD). In this spectroscopic system, a five-branch fiberscope is used. Each objective lens has a different narrow-band optical filter for the hydrogen Balmer lines and background continuum radiation. The electron density and temperature in a plasmoid can be obtained from the intensity ratio measured with these filters. The electron density distribution in the range of 10^{22} and 10^{24} m^{-3} and the temperature distribution of around 1 eV are observed. The dependence of the pellet ablation on the magnetic field strength is investigated.

1. Introduction

Solid hydrogen pellet injection is a primary technique for efficient core plasma fuelling in magnetic fusion devices. The pellet ablation and subsequent behavior of the dense plasmoid (ionized ablation cloud) are key elements to determine the characteristics of pellet refuelling. The behavior of the plasmoid is rather complicated due to its interaction with the background plasma and the magnetic field. A quantification of the internal distribution in the plasmoid is helpful for the understanding of these behaviors.

In the Large Helical Device (LHD), the electron density distribution of the plasmoid was obtained by imaging measurements using a bifurcated fiberscope [1]. Here, it was assumed that the electron temperature of the plasmoid is in the limited narrow range. To evaluate the internal distribution precisely, it is essential to identify not only the electron density but also the electron temperature of the plasmoid.

In this paper, we apply a fast imaging spectroscopy with high spatiotemporal resolution using a five-branch fiberscope and a fast camera to identify both the electron density and temperature distributions in the plasmoid. We also discuss the dependence of the distribution in the plasmoid on magnetic field strength.

2. Experimental Setup

The spectra of hydrogen Balmer-lines and background continuum radiation are determined by the electron density and temperature of the plasmoid. Here, the emission from the background plasma can be ignored, because the density of the plasmoid is several hundred times greater than that of the background plasma.

In this study, it should be noted that the spectra are estimated from fitting with the theoretical data. In the theoretical data, the intensity of the spectra is calculated on the assumption of local thermodynamic equilibrium. The broadening profile of the spectra is calculated using Ref. [2]. The spectra can be estimated from the intensity ratio measured using narrow-band optical filters having different wavelengths and bandwidths. We concentrate on the Balmer-β line (wavelength: 486.1 nm) and Balmer-γ line (wavelength: 435.8 nm) to evaluate the electron density and temperature of the plasmoid. The Balmer-α line and background continuum radiation are also measured as a reference and the plasma thickness can be probably obtained by evaluation of the effect of self-absorption in the Balmer-α line. The density and temperature distribution of the plasmoid is uniquely determined from the intensity ratio of the filters.

In this spectroscopic system, a five-branch fiberscope is used. The scope is composed of

15,000×5 quartz fiber elements packed in a flexible protective tube made of stainless-steel. Each objective lens has a field of view of 15 degrees. The five images through the different filters are focused onto a single fast camera so that the simultaneity is ensured. The fast camera is equipped with a 12-bit SR-CMOS sensor. The plasmoid can be observed close behind the pellet injection port. The pellet is injected into the NBI plasma. The nominal pellet size is 3.4 mmφ×3.4 mmℓ. The typical pellet speed is 1,200 m/s.

3. Results

Figure 1 shows the electron density and electron temperature imaging in the plasmoid. It seems that the plasmoid of about 0.1 m in size expands in a direction parallel to the magnetic field line. We confirmed that the electron density distribution is in the range between 10^{22} and 10^{24} m^{-3} and the temperature distribution is about 1 eV, indicating that a weakly-ionized plasmoid is observed. These results are in agreement with global spectroscopic measurements [3].

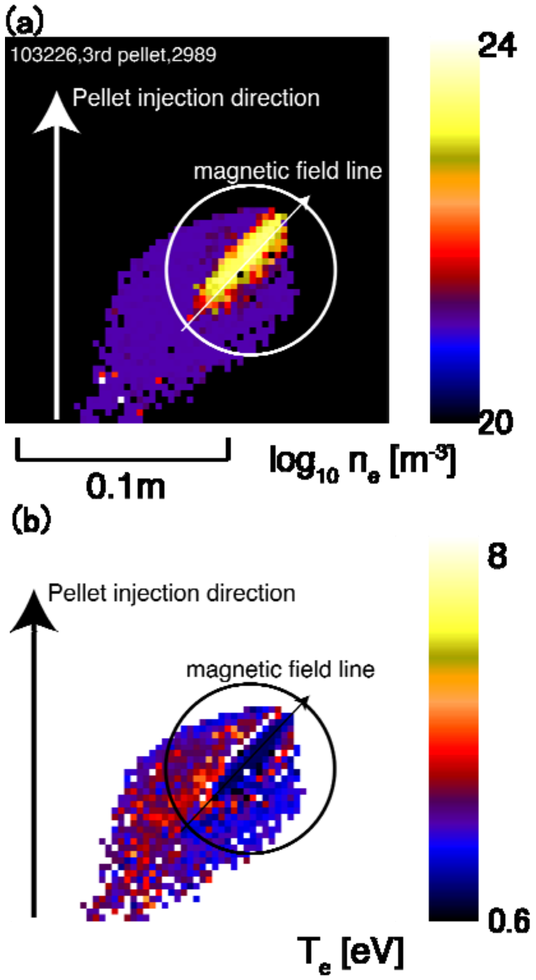

Fig.1. (a) Electron density imaging and (b) electron temperature imaging.

Figure 2 shows the dependence of the penetration depths of pellets on magnetic field strength. The penetration depth is shallower at lower magnetic field, suggesting that the electron density distribution in the plasmoid might depend on the magnetic field strength. In an RFP, an enhancement of particle diffusion at low magnetic field resulting in higher ablation has been observed [4]. The difference in the density distribution in the plasmoid between low and high magnetic field will be shown in the near future.

Acknowledgments

This study was partly supported by Grant-in-Aid for Young Scientists (B) (No.21760694) and Grant-in-Aid for Scientific Research (S) (No. 20226018), by the Sasakawa Scientific Research Grant from The Japan Science Society and by NIFS10ULPP017 from the budget grant-in-aid of the National Institute for Fusion Science.

References

[1] G. Motojima *et al.*, Plasma. Fusion Res. **5**, S1033 (2010).

[2] C. Stehle and R. Hutcheon, Astron. Astrophys. Suppl. Ser. **140**, 93 (1999).

[3] M. Goto *et al.*, Plasma Phys. Control. Fusion **49**, 1163 (2007).

[4] A. Canton *et al.*, Plasma Phys. Control. Fusion **43**, 225 (2001).

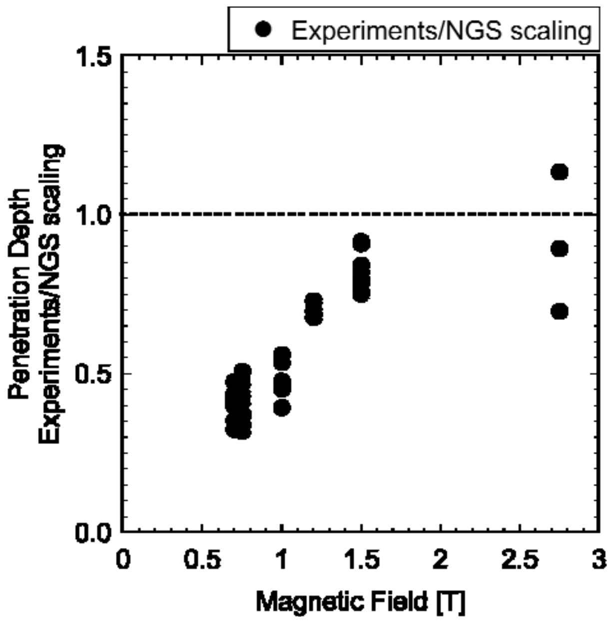

Fig.2. Penetration depth as a function of magnetic field strength. The experimental penetration depth is normalized by the prediction by NGS scaling. The central electron temperature is the same (1 keV) for each data point.